The glutamate transporter EAAT5 works as a presynaptic receptor in mouse rod bipolar cells

Eric Wersinger[1], Yannick Schwab[2], José-Alain Sahel[1,2,3], Alvaro Rendon[1], David V. Pow[5], Serge Picaud[1,3] and Michel J. Roux[1]

[1]*Laboratory of Cellular and Molecular Physiopathology of the Retina, National Institute for Health and Medical Research (INSERM Unité 592), Université Pierre et Marie Curie-Paris6, Paris, France*
[2]*IGBMC, 1 rue Laurent Fries BP10142, 67404 Illkirch cedex, France*
[3]*Fondation Ophtalmologique A. de Rothschild, Paris, France*
[4]*Centre National d'Ophtalmologie des quinze-vingts, Paris, France*
[5]*School of Biomedical Sciences, University of Newcastle, New South Wales, Australia*

Membrane neurotransmitter transporters control the concentration of their substrate in the synaptic clefts, through the thermodynamic coupling of uptake to the movement of Na^+ and other ions. In addition, excitatory amino acid transporters (EAAT) have a Cl^- conductance which is gated by the joint binding of Na^+ and glutamate, but thermodynamically uncoupled to the flux of glutamate. This conductance is particularly large in the retina-specific EAAT5 isoform. In the mouse retina, we located EAAT5 in both cone and rod photoreceptor terminals and in axon terminals of rod bipolar cells. In these later cells, application of glutamate on the axon terminal evoked a current that reversed at E_{Cl}, was insensitive to bicuculline, TPMPA, strychnine, DL-AP5, CNQX and MCPG, but blocked by the glutamate transporter inhibitor DL-tBOA. Furthermore, short depolarizations of the bipolar cells evoked a DL-tBOA and Cd^{2+}-sensitive current whose amplitude was comparable to the glutamate-evoked current. Its kinetics indicated that EAAT5 was located close to the glutamate release site. For 2 ms depolarizations evoking maximal responses, the EAAT5-mediated current carried between 2 and 8 times more charge as an average inhibitory GABA or glycine postsynaptic current received spontaneously from amacrine cells, with 10 mM or 0.5 mM intracellular EGTA, respectively. In conditions for which reciprocal inhibition could be monitored, the charge carried by the EAAT5 current was 1.5 times larger than the one carried by the inhibitory postsynaptic currents received from amacrine cells. These results indicate that EAAT5 acts as a major inhibitory presynaptic receptor at mammalian rod bipolar cell axon terminals. This feedback mechanism could control glutamate release at the ribbon synapses of a non-spiking neuron and increase the temporal contrast in the rod photoreceptor pathway.

(Resubmitted 29 July 2006; accepted 7 September 2006; first published online 14 September 2006)
Corresponding author M. J. Roux : IGBMC-ICS, 1 rue Laurent Fries BP10142, 67404 Illkirch cedex, France.
Email: mjroux@igbmc.u-strasbg.fr

Through their buffering and uptake capacities, neurotransmitter transporters help shape synaptic events, especially when release levels are high, and limit neurotransmitter spill-over between neighbouring synapses. Transporters can also have roles beyond the control of the extracellular and intracellular neurotransmitter concentrations, by modulating neuronal activity through their electrogenic properties. First, neurotransmitter uptake is tightly coupled to the flux of ions. Depending on the transport stoichiometry, this usually generates a transport-associated current of small amplitude, but which still can have a direct influence on the cell excitability as recently shown for postsynaptic GAT-1 (Bagley *et al.* 2005). Second, transporters can behave as neurotransmitter-gated ionic channels (reviewed in Sonders & Amara, 1996). This is particularly relevant for the glutamate transporters EAAT4 (Fairman *et al.* 1995) and EAAT5 (Arriza *et al.* 1997), which both have a large Cl^- conductance gated by Na^+ and glutamate. Such a Cl^- conductance with the pharmacological characteristics of glutamate transporters was first demonstrated in salamander and turtle cone photoreceptors (Sarantis *et al.* 1988; Tachibana & Kaneko, 1988; Eliasof & Werblin, 1993; Picaud *et al.* 1995*b*) and subsequently reported in salamander rod photoreceptors (Grant & Werblin, 1996), teleost retinal bipolar cells (Grant & Dowling,

 DOI: 10.1113/jphysiol.2006.118281

1995, 1996; Palmer *et al.* 2003; Wong *et al.* 2005) as well as at an invertebrate neuromuscular junction (Dudel & Schramm, 2003) and in mammalian cerebellar Purkinje cells (Otis *et al.* 1997; Auger & Attwell, 2000). Thanks to this neurotransmitter-gated conductance, glutamate transporters act as a presynaptic receptor enabling the cell to measure its own glutamate release in salamander cone photoreceptors (Picaud *et al.* 1995*a*) and goldfish bipolar cells (Palmer *et al.* 2003). An extrasynaptic location (Dehnes *et al.* 1998) and the small amplitude of its current compared to AMPA postsynaptic currents suggest that EAAT4 is a key element in glutamate clearance at the parallel fibre/Purkinje cell synapse rather than a postsynaptic receptor (Otis *et al.* 1997; Auger & Attwell, 2000). In addition, glutamate transporters have been shown to contribute significantly as postsynaptic receptors to the light response in teleost retinal bipolar cells (Grant & Dowling, 1995, 1996; Wong *et al.* 2005).

To determine whether glutamate transporters may play similar function in the mammalian retina, EAAT5 was located in mouse retinal sections and responses to glutamate were recorded in mouse bipolar cells. EAAT5 was expressed in the synaptic terminals of photoreceptors (cones and rods) and rod bipolar cells. A glutamate transporter current reversing at E_{Cl} was recorded from rod bipolar cells, with a major contribution of the axon terminals. It could be elicited by triggering glutamate release through depolarization of the recorded cell, suggesting that EAAT5 acts as a presynaptic receptor in mouse rod bipolar cells. The charge carried by this current was 1.5 time larger than the one carried by the reciprocal inhibition received from amacrine cells, indicating that the feedback mediated by presynaptic EAAT5 plays a major role in controlling the output from rod bipolar cells.

Methods

Retinal slice preparation

Mice strains used in this study were either of the C57BL/6J or Balb/c ByJ or crosses between them, purchased (pure strains) from Charles River (Lyon, France) or bred (crosses) at the Mouse Clinical Institute animal house (Illkirch, France). Procedures involving animals and their care were conducted in agreement with the French Ministry of Agriculture and the European Community Council Directive no. 86/609/EEC, OJL 358, 18 December 1986. Adult (9–19 weeks) mice were killed by cervical dislocation. The eyes were enucleated and immediately put in ice-cold bicarbonate-buffered saline (BBS), composed of (mM): NaCl 126, KCl 2.5, $CaCl_2$ 2.4, $MgCl_2$ 1.2, NaH_2PO_4 1.2, $NaHCO_3$ 18, glucose 11 previously bubbled with 95% O_2–5% CO_2. The cornea, lens and vitreous humor were removed. The retina was detached from the pigmented epithelium and embedded in agarose (1.5%) prepared in phosphate-buffered saline (PBS) (0.1 M; pH 7.4) kept at 42°C. After agarose solidification on ice, the retina was cut in 150 or 200 μm thick slices using a Leica VT1000S vibratome (Leica, Wetzlar, Germany). The slices were kept at room temperature in bubbled BBS for at least half an hour before recordings.

Bipolar cell recordings

Slices were observed under infrared differential interference contrast (DIC) using a ×63 objective and a Hamamatsu C8484 camera on a Leica DMLFS microscope. The preparation was continuously perfused at $\sim$2 ml min^{-1} with bubbled BBS. Pipettes (6–8 MΩ) were pulled from GC150TF borosilicate glass capillaries (Harvard Apparatus) on a horizontal puller (DMZ Universal Puller, Zeitz Instrumente, Munich, Germany). Four different intracellular solutions were used. Two contained 10 mM EGTA-Na_4, and either (mM) KCl 42, K-gluconate 98, $MgCl_2$ 1, EGTA-Na_4 0.5, Hepes 5, ATP-Na_2 5 ($E_{Cl} = -28.9$ mV, junction potential of 12.4 mV), or KCl 138, $MgCl_2$ 3, $CaCl_2$ 1, Hepes 10, ATP-Na_2 3, GTP-Na_3 0.5 ($E_{Cl} = 1.9$ mV, junction potential of 3.9 mV). These solutions will be referred to as $E_{Cl} = -29$ mV and $E_{Cl} = 2$ mV, respectively. The $E_{Cl} = 2$ mV solution was used for most of the experiments presented here. Another solution containing 0.5 mM EGTA was otherwise identical to the $E_{Cl} = 2$ mV solution. Finally, a Cs-based solution with very low EGTA (0.1 mM) was used to monitor reciprocal inhibition from amacrine cells. It contained (mM): CsCl 125, $MgCl_2$ 1, TEA-Cl 15, EGTA- Na_4 0.1, glutamic acid 5, Hepes 10, ATP-Na_2 3 and GTP-Na_3 0.5. All solutions contained 10 μM of Alexa Fluor (488 or 594) hydrazide (Molecular Probes, Eugene, OR, USA), and pH was adjusted to 7.4 with NaOH or CsOH. Potentials were corrected post-recording for the calculated junction potential. For simplicity, potentials indicated in the text are rounded to integer values. All experiments were performed at room temperature (20–25°C). Data were acquired using a Multiclamp 700A amplifier, a Digidata 1322A interface and the pCLAMP9 software (Molecular Devices, Sunnyvale, CA, USA). Data were filtered prior to digitization at a frequency of 1/2 or 1/5th of the acquisition frequency, which was 200 Hz for puffed glutamate experiments and 10 kHz for depolarizing pulse experiments. Agonists and antagonists were applied either through bath application or locally with a puff pipette connected to a Picospritzer III (Parker Hannifin, Fairfield, NJ, USA). DL-Threo-β-benzyloxyaspartate (DL-tBOA), 1,2,5,6-tetrahydropyridin-4-yl)methylphosphinic acid (TPMPA) and 6-cyano-7-nitroquinoxaline-2,3-dione (CNQX) were obtained from Tocris (Ellisville, MI, USA); all others chemicals were obtained from Sigma-Aldrich (Lyon, France).

All values are indicated as means ± S.E.M.

Immunohistochemistry

Retinas from C57BL6/J mice were obtained from animals (8-weeks old) that had been killed by an overdose of sodium pentobarbital (200 mg kg^{-1}, I.P.). Retinas were fixed by immersion with 4% paraformaldehyde in 0.1 M phosphate buffer, pH 7.4 for a duration varying between 5 min and 2 h. Vibratome sections (40 μm thick) were then cut and labelled using standard protocols, with a EAAT5 rabbit antiserum (dilution 1/5000) previously characterized (Pow & Barnett, 2000; Pow *et al.* 2000). Labelling was detected using biotinylated secondary antibodies, streptavidin–horseradish peroxidase complex, and revealed using diaminobenzidine as a chromogen. Immunolabelled sections were viewed using a Zeiss Axioskop.

Results

EAAT5 localization in the mouse retina

In the mouse retina, EAAT5 immunolabelling was strongly dependent on the duration of fixation. For fixation times (between 5 and 20 min), cells in the inner nuclear layer with the characteristic shape of rod bipolar cells (RBCs) were labelled (Fig. 1*A* and *B*) from dendrites to axon terminals, with a stronger signal in the axon terminals (Fig. 1*B*). Double immunolabelling with the RBC specific marker PKCα confirmed the expression of EAAT5 in RBC (see accompanying online supplemental material, Supplemental Fig. 1). A diffuse staining was observed in the outer plexiform layer (OPL), which could correspond to RBC dendrites or photoreceptor terminals. For longer fixation times (2 h), the RBC labelling was strongly reduced, limited to the axon terminals (Fig. 1*C*). In contrast, the OPL staining was much stronger and could be attributed to photoreceptor terminals (Fig. 1*C*). The labelling pattern included small rounded terminals and larger, more heavily stained terminals in the inner part of the OPL, suggesting that both rod and cone terminals expressed EAAT5.

Exogenous glutamate evokes a transporter current in rod bipolar cell axon terminals

To test if EAAT5 could carry a detectable current in the mouse retina, whole-cell patch-clamp recordings were obtained from RBCs in adult mouse retinal slices. Recorded cells were chosen in the two outer rows of cell bodies of the inner nuclear layer. Cell identification was established post-recording, based on the morphology revealed by the Alexa dye included in the intracellular solution, according to the classification of Ghosh *et al.* (2004): only cells with an axon ending in the inner part of the IPL and terminating in a small group of fat varicosities were considered for further analysis (Fig. 2*A*). Puff-application (100 ms) of glutamate (1 mM)

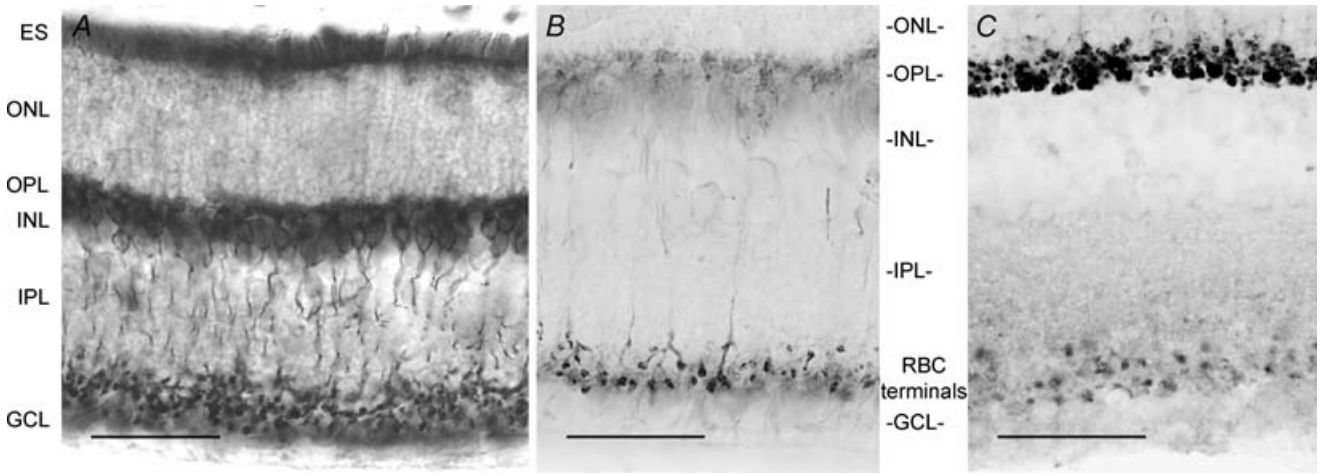

Figure 1. The glutamate transporter EAAT5 is expressed in rod bipolar cells and photoreceptor terminals
A and *B*, section of a mouse retina fixed for 20 min immunolabelled for EAAT5. Staining is found in rod bipolar cells, especially in their axon terminals as can be better seen in the less exposed image in *B*. *C*, section of a mouse retina fixed for 2 h immunolabelled for EAAT5. Axon terminals of RBCs are more diffusely labelled, while a distinct staining of rod and cone photoreceptor terminals can now be seen in the OPL. The scale bars represent 60 μm in *A*, and 30 μm in *B* and *C*. ES: external segments; ONL: outer nuclear layer; OPL: outer plexiform layer; INL: inner nuclear layer; IPL: inner plexiform layer; GCL: ganglion cell layer.

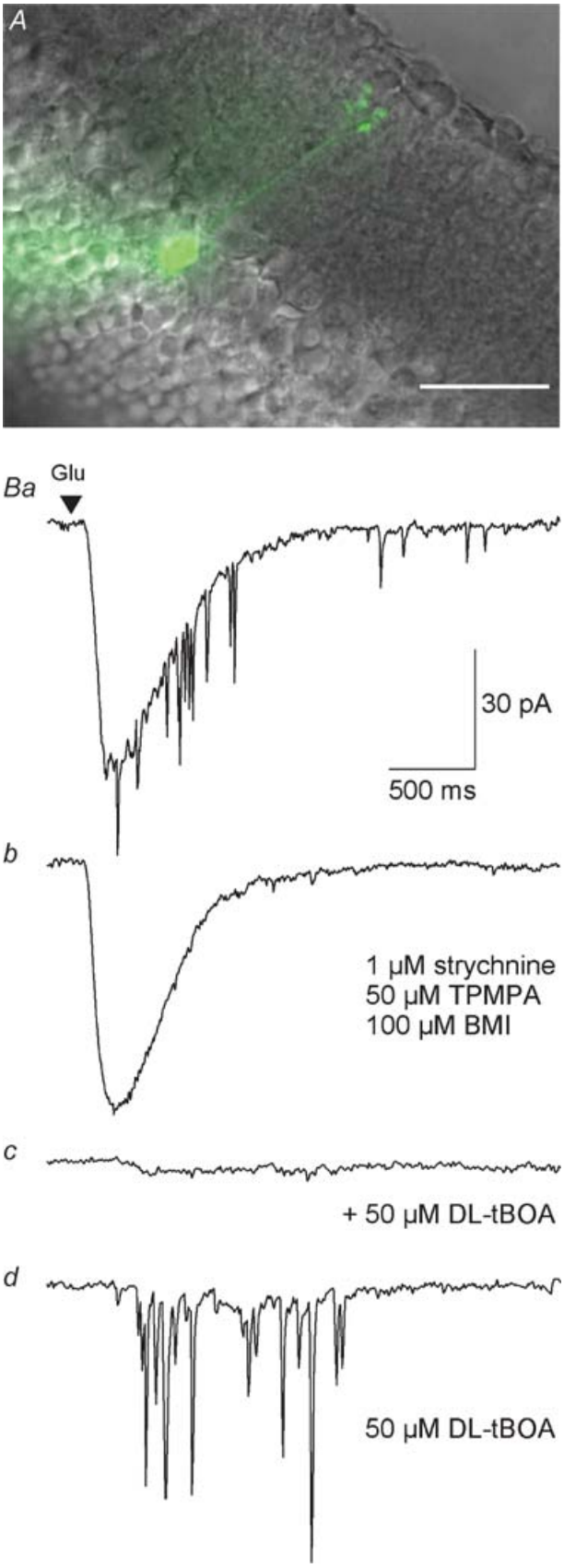

in the vicinity of the axon terminal evoked a transient and slowly decaying inward current (I_{Glu}) (Fig. 2*Ba*). I_{Glu} could not be attributed to a mechanical artefact due to the puff itself, as applications of BBS + 2 mM sucrose did not evoke any current ($n = 6$, data not shown). In addition, fast inward postsynaptic currents were often seen on top of I_{Glu} (Fig. 2*Ba*), as expected from the known inputs from both GABAergic and glycinergic amacrine cells on RBC terminals. These synaptic events were fully blocked by a cocktail of ionotropic glycine and GABA (A and C) receptor inhibitors (1 μM strychnine, 100 μM bicuculline methiodide and 50 μM TPMPA), leaving the slow phase unaffected (Fig. 2*Bb*, $n = 5$). They were also blocked by a cocktail of glutamate receptor inhibitors (50 μM CNQX, 50 μM DL-2-amino-5-phosphonovaleric acid (DL-AP5), 500 μM (RS)-α-methyl-4-carboxyphenylglycine (MCPG)), which had no effect on the slow phase (data not shown, $n = 5$). This dual pharmacology was expected for inhibitory postsynaptic currents (IPSCs) as the amacrine cells are depolarized by glutamate. The absence of effect on the slow phase excluded that I_{Glu} could be due to the direct activation of glutamate ionotropic receptors, to the indirect activation of GABA or glycine receptors, or to the modulation of a conductance via activation of metabotropic glutamate receptors.

Following the demonstration of the EAAT5 localization in RBC axon terminals, we checked if a glutamate-transporter current could contribute to I_{Glu}. The non-selective glutamate transporter inhibitor DL-threo-β-benzyloxyaspartate (DL-tBOA) (75 μM) was puff-applied (10 s) just prior to the glutamate application. In the presence of the inhibitory receptor inhibitor cocktail (1 μM strychnine, 50 μM TPMPA and 100 μM bicuculline methiodide), the slow inward current disappeared quasi-completely (Fig. 2*Bc*), indicating that I_{Glu} was due to the activity of glutamate transporters ($n = 3$). Moreover, when DL-tBOA was applied alone, it suppressed only the slow inward current while the faster synaptic-like currents could still be seen, at a higher frequency than in control conditions ($n = 3$, Fig. 2*Bd*). This later result can

Figure 2. Glutamate-evoked current in rod bipolar cell axon terminals
A, morphology of a recorded rod bipolar cell filled with Alexa Fluor 488 hydrazide, superimposed to the DIC image of the retinal slice; scale bar = 40 μM. *B*, puffs of glutamate (100 ms, 1 mM) in the vicinity of the axon terminals of a rod bipolar cell evoked a transient and slow current as well as IPSCs (*Ba*). These fast synaptic events could be blocked by the joint application of inhibitors of glycine (strychnine, 1 μM), $GABA_A$ (bicuculline methiodide, 100 μM) and $GABA_C$ receptors (TPMPA, 50 μM), while the slow phase of the response was not affected (*b*). Application of the glutamate transporter inhibitor DL-tBOA (75 μM) blocked the slow phase either when applied in conjunction with inhibitory receptor blockers (*c*) or alone (*d*). ($E_{Cl} = 2$ mV, cell held at −74 mV).

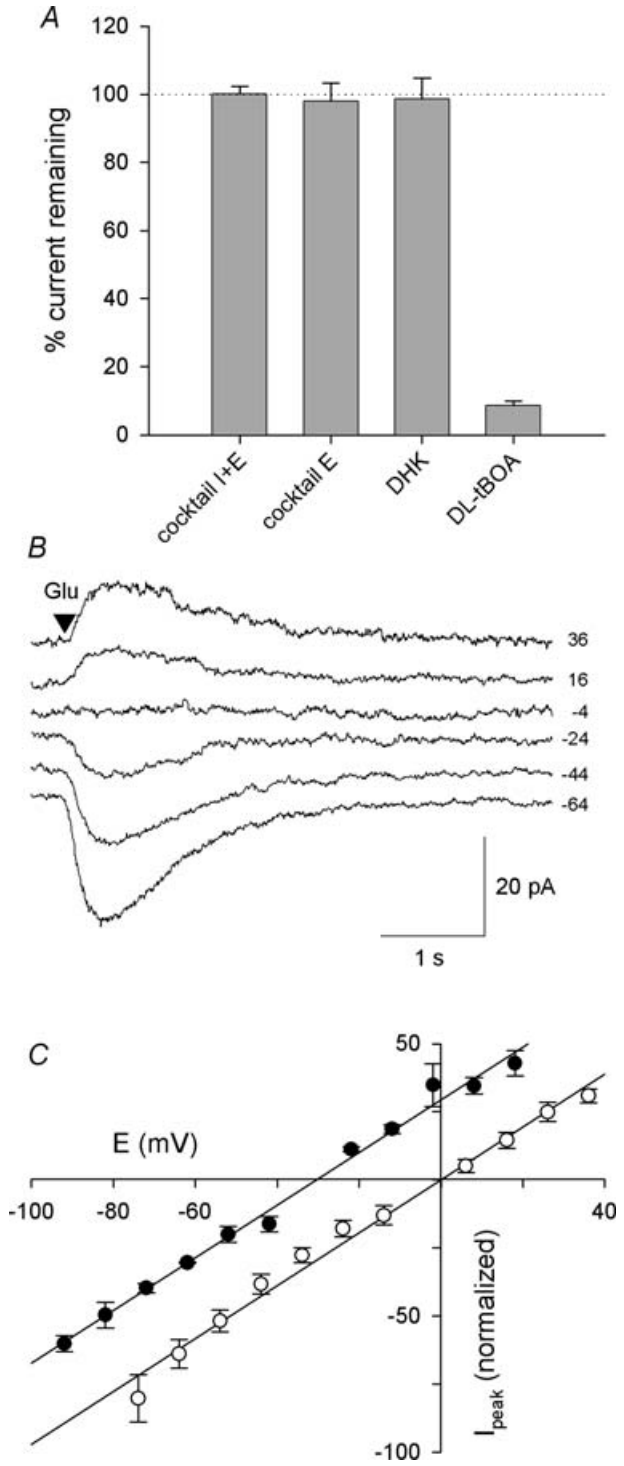

Figure 3. Pharmacology and reversal of the glutamate-induced current

A, percentage of the remaining glutamate-induced current in the presence of various inhibitors. Cocktail I + E is a mix of inhibitors of both excitatory and inhibitory ionotropic receptors (50 μM CNQX, 50 μM DL-AP5, 100 μM bicuculline methiodide, 50 μM TPMPA and 1 μM strychnine), while cocktail E is mix of inhibitors of ionotropic and metabotropic glutamate receptors (50 μM CNQX, 50 μM DL-AP5, 500 μM MCPG). The concentrations used were 500 μm for dihydrokainte (DHK), 50 μM for DL-tBOA. Currents were evoked by a glutamate puff (100 ms, 1 mM) in the vicinity of RBC axon terminals. All drugs were bath applied. *B*, currents evoked by glutamate (1 mM, 100 ms puffs) at various holding potentials, from −64 mV to 36 mV, in 20 mV steps. *C*, peak amplitude of the glutamate-evoked current as a function of the holding potential, obtained either for $E_{Cl} = -29$ mV (●, $n = 6$) or $E_{Cl} = 2$ mV (○, $n = 9$). Data were normalized to the slope of the linear regression for each cell. The cells considered in *A–C* did not receive spontaneous GABAergic and/or glycinergic inputs to facilitate determination of the response peak.

be expected from the inhibition of glutamate transporters in the vicinity of the recorded cell, as the subsequent increase in the extracellular glutamate concentration should lead to a stronger depolarization of the amacrine cells contacting the recorded RBC.

The slow phase of the glutamate response was further characterized on RBCs for which no spontaneous or glutamate-evoked synaptic currents were recorded. This kind of glutamate response was frequently encountered when the axon terminals were near the surface of the slice. In these cells, the mean peak amplitude of I_{Glu} was -28.8 ± 4.1 pA ($n = 15$) at a holding potential of -64 mV (intracellular solution $E_{Cl} = 2$ mV), with individual values ranged from -13.3 to -61.6 pA. The glutamate transporter agonist D-aspartate (1 mM) also induced an inward current (-26.2 ± 5.1; $n = 9$). As expected from the results obtained from cells receiving synaptic inputs shown in Fig. 2, I_{Glu} was blocked at $91.5 \pm 1.5\%$ ($n = 13$) by bath application of 50 μM DL-tBOA, confirming that the slow phase was due to the activation of glutamate transporters (Fig. 3*A* and Supplemental Fig. 2*a*). Dihydrokainate (500 μM) did not have any effect ($1.3 \pm 6.0\%$ of current diminution, $n = 6$), indicating that the EAAT2 isoform was not contributing to I_{Glu} (Fig. 3*A* and Supplemental Fig. 2*b*). I_{Glu} was unaffected by a bath-applied cocktail of blockers: 1 μM strychnine, 100 μM bicuculline methiodide, 50 μM TPMPA, 50 μM CNQX and 50 μM DL-AP5 ($100.1 \pm 2.1\%$ of current remaining, $n = 9$) or 50 μM CNQX and 50 μM DL-AP5 + 500 μM MCPG ($97.9 \pm 5.4\%$ of current remaining, $n = 14$) (Fig. 3*A* and Supplemental Fig. 2*c*).

In order to verify that the glutamate-evoked current was indeed due to the Cl^- conductance of EAAT5, the reversal potential of I_{Glu} was determined for two distinct E_{Cl} conditions, puffing glutamate while holding the cell at various holding potentials. Representative traces for $E_{Cl} = 2$ mV are shown in Fig. 3*B*. I_{Glu} was found to reverse at -29.6 ± 1.3 mV ($n = 6$) when $E_{Cl} = -29$ mV and at -0.4 ± 2.0 mV ($n = 9$) when $E_{Cl} = 2$ mV, indicating that I_{Glu} corresponded mostly to the Cl^- conductance associated to glutamate transporters and not to a current generated by glutamate uptake. In both cases, the current to voltage relationships were linear on the studied voltage range (Fig. 3*C*).

Exogenous glutamate evokes a transporter current from the rod bipolar cell soma/dendrites

A contribution of a transporter current in the response to the glutamate released by photoreceptors has been reported in the ON cone or mixed input bipolar cells in the teleost retina (Grant & Dowling, 1995, 1996). Looking for a comparable contribution in mouse rod bipolar cell, we applied glutamate at the level of the outer plexiform layer above the recorded cell. Puffs of glutamate (5 ms, 1 mM) evoked a small inward current peaking at -4.6 ± 0.5 pA ($n = 9$) at -64 mV, which was blocked by 75 μM DL-tBOA ($79.0 \pm 2.6\%$ of current diminution, $n = 6$ data not shown). When progressively increasing the puff duration from 5 to 50 ms, a secondary peak of larger maximal amplitude developed (Supplemental Fig. 3*a*), suggesting that longer puffs activated both dendritic/somatic and axonal transporters, the larger component coming from the axonal compartment. This was supported by the comparable time course of currents evoked by 100 ms glutamate puffs applied either above the dendritic arbor or the axon terminals of a given RBC (Supplemental Fig. 3*a*), and by the fact that some potential RBCs, whose axons were cut during the slicing procedure, presented similar responses to glutamate ($n = 3$). Due to its small amplitude and the difficulty to isolate it from the larger axonal component, this dendritic and/or somatic EAAT5 current was not studied further.

Transient transporter current following depolarization

To examine whether glutamate transporters could act as presynaptic receptors, calcium-dependent vesicular release of glutamate was evoked from the recorded RBC by short depolarizations. Paired-pulse stimulations were used to obtain additional information on the release properties of these RBC terminals (pairs of 2 ms voltage jumps from -84 to -24 mV, 100 ms apart). A transient inward current (I_{trans}) followed the fast capacitive current upon repolarization (Figs 4, 5 and 6). In addition, as for responses to glutamate puffs, IPSCs were frequently seen (Fig. 4).

Puff application of 75 μM DL-tBOA blocked the inward current following depolarization, while postsynaptic currents were still observed (Fig. 4*A*). In agreement with this complete block by DL-tBOA, puff application of 1 μM strychnine + 50 μM TPMPA + 100 μM bicuculline methiodide did not affect I_{trans} while completely suppressing IPSCs (Fig. 4*B*). I_{trans} amplitudes for the first and second pulses were, respectively, $101.6 \pm 2.3\%$ and $104.6 \pm 2.9\%$ of control ($n = 20$) (Fig. 4*B*). In the following characterization, none of the ionotropic receptor blockers were added to the bath solution: some IPSCs were superimposed on I_{trans} (see Fig. 4*B*), but such events were rare and did not hinder the measurement of I_{trans}.

I_{trans} ran down quickly over time and could rarely be detected after 3 min following establishment of the whole-cell configuration (Fig. 5*C*), in a similar fashion to what has been reported from the large terminals of goldfish bipolar cells (Palmer *et al.* 2003). The run-down time courses were identical for the first and second pulses (data not shown). Run-down of I_{trans} was not due to inactivation/internalization of the transporters, as I_{Glu} could still be evoked with comparable amplitude after complete disappearance of I_{trans} (data not shown). In fact, it may correspond to a depletion of the vesicular pool: following an apparent complete run-down after trains of 2 ms paired-pulses at 5 s intervals, I_{trans} could frequently be re-observed after a few minutes without depolarization.

To circumvent this limitation, depolarizations were applied quickly after the passage in whole-cell, to maximize the recording time for I_{trans}. In doing so, I_{trans} could be recorded in a large majority of the tested RBC (93%, 331 out of 355). On the contrary, I_{trans} was not observed in any of the 25 cone bipolar cells patched in this study. All the pharmacological tests were performed using puff applications in the vicinity of the RBC axon terminals. While the exact concentration of the applied drug reaching the terminal could not be known, this method allowed for a fast wash of the antagonist compatible with the observed run-down of I_{trans}. Figure 5*A* shows traces of the current evoked by paired depolarizations before (black trace), at the end of (dark grey trace), and 1 min after application of 75 μM DL-tBOA (light grey trace). To determine the DL-tBOA-sensitive fraction of I_{trans}, the zero current was estimated as being reached after more than 3 min in the whole-cell configuration. Puff applications of 75 μM DL-tBOA (between 100 ms and 2 s, dark grey trace) blocked I_{trans} at $97.6 \pm 1.23\%$ for the first peak, and at $94.8 \pm 1.4\%$ for the second peak ($n = 9$) (see percentage of remaining current in Fig. 4*C*). I_{trans} quickly recovered its initial amplitude (light grey trace). When glutamate (1 mM) was applied locally with a puff pipette, I_{trans} was completely suppressed following the depolarization (Fig. 5*D*, dark grey trace). Although the peak amplitude of I_{trans} was always smaller ($65.2 \pm 4.8\%$, $n = 9$) than the steady-state current evoked by the application of glutamate, it could be as large as 88% of the amplitude of the glutamate-induced current. These observations suggested that I_{trans} was produced by the glutamate transporter mediating I_{Glu} characterized above. In addition, I_{trans} was not affected by glutamate receptor blockers ($97.3 \pm 0.9\%$ remaining current in the presence of 50 μM CNQX, 50 μM DL-AP5 and 500 μM MCPG, $n = 5$).

The DL-tBOA-sensitive current was isolated by subtraction for kinetic analysis (Fig. 5*B*). When the cell was held at -84 mV, a 2 ms pulse to -24 mV evoked a current of -32.7 ± 3.5 pA ($n = 11$). I_{trans} peaked 5.6 ± 0.1 ms ($n = 11$) after the start of the depolarization, and

decayed with a time constant of 10.2 ± 0.4 ms ($n = 11$). A second pulse 100 ms later evoked a smaller current (-14.5 ± 1.4 pA, $n = 11$). The amplitude ratio of the second pulse compared to the first was on average 0.46 ± 0.02 ($n = 11$). However, the kinetic parameters of the second pulse were similar to those of the first one, as it peaked 6.6 ± 0.3 ms ($n = 11$) after the start of the depolarization and decayed with a time constant of 9.1 ± 0.6 ms ($n = 11$).

I_{trans} dependence on Ca^{2+} channel current

When the voltage of 2 ms depolarizing pulses was varied, current could be detected from -50 mV

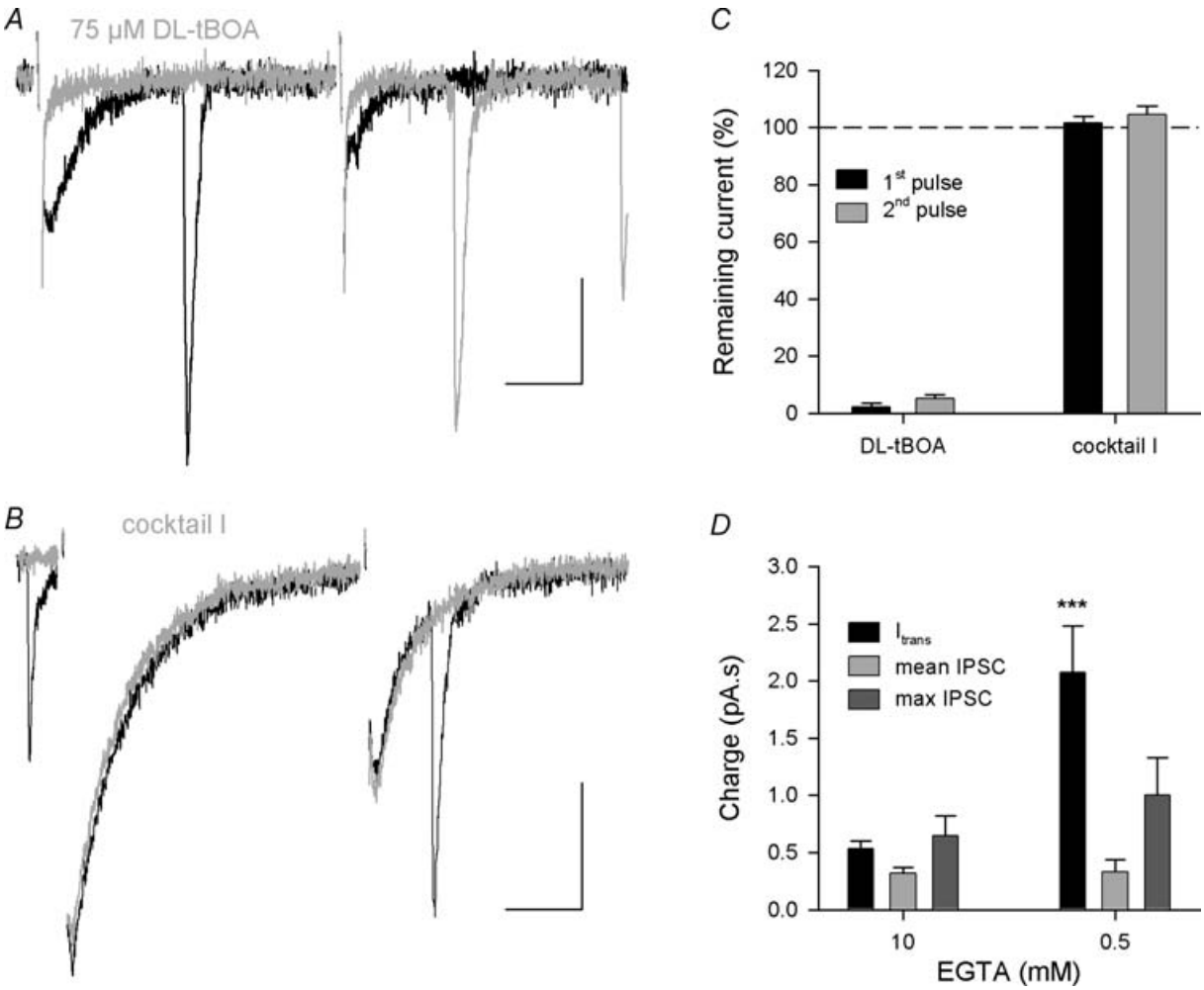

Figure 4. Depolarizations evoke a transient glutamate transporter current in rod bipolar cells
Paired (100 ms apart) 2 ms depolarizations from -84 mV to -24 mV were given every 5 s. A transient current (I_{trans}) was observed following each depolarization, partially merged in the capacitive transient (*A* and *B*). In addition, faster decaying synaptic-like currents were recorded with various delays compared to the depolarization, some of them preceding the depolarization (control trace in *B*). *A*, the glutamate transporter inhibitor DL-tBOA (75 μM) blocked reversibly I_{trans} but not the synaptic events (grey trace superimposed to the black control trace). For this cell, the intracellular solution contained 10 mM EGTA. Scale bars represent 25 ms and 30 pA. *B*, a cocktail blocking both GABA and glycine ionotropic receptors (1 μM strychnine + 50 μM TPMPA + 100 μM bicuculline methiodide) did not affect I_{trans} but blocked completely the IPSCs (grey trace superimposed on the black control trace). For this cell, the intracellular solution contained 0.5 mM EGTA. Scale bars represent 25 ms and 50 pA. For clarity, most of the capacitive transient has been masked in *A* and *B*. *C*, summary of the inhibition par 75 μM DL-tBOA ($n = 9$) and the inhibitory cocktail ($n = 20$) on the amplitude of I_{trans} following the 1st (black) and 2nd pulse (grey). *D*, mean charge carried by I_{trans} following the 1st pulse (black) compared to the charge of a mean IPSC (light grey) or of the largest IPSC (dark grey) for two concentrations of intracellular EGTA ($n = 10$ cells for 10 mM, $n = 6$ cells for 0.5 mM EGTA). While the I_{trans} charge was significantly increased ($P = 0.0003$) when switching from 10 mM to 0.5 mM, it was not the case for the charge carried by the mean ($P = 0.91$) or max IPSCs ($P = 0.31$).

upward (Fig. 6*A*–*C*). The peak amplitude of the first and second pulses as a function of the depolarization voltage could be fitted to a Boltzmann distribution, with half-potentials of -42.0 ± 1.1 mV and -43.4 ± 1.1 mV, respectively ($n = 7$). This voltage dependence of I_{trans}, similar to that of L-type voltage-gated Ca^{2+} channels reported from mouse bipolar cells (Berntson *et al.* 2003), suggested that I_{trans} was due to glutamate release from the recorded cell. While the weaker depolarizations induced responses of comparable amplitudes for the first and second pulses, with weak paired-pulse facilitation below -44 mV, a marked paired-pulse depression was observed from -40 mV upward.

As additional evidence that I_{trans} was subsequent to synaptic release, we tested its dependence upon Ca^{2+} currents. Puff application (10 s) of 100 μM Cd^{2+} next to the axon terminal strongly reduced I_{trans} (Fig. 6*D*, $n = 4$). In paired pulse experiments as described above, the first peak was reduced by $86.5 \pm 2.3\%$, the second by $80.0 \pm 3.9\%$ ($n = 4$). Moreover, when recordings were performed in Ca^{2+}-free BBS, no I_{trans} could be detected, while the cell did respond to puff applications of 1 mM

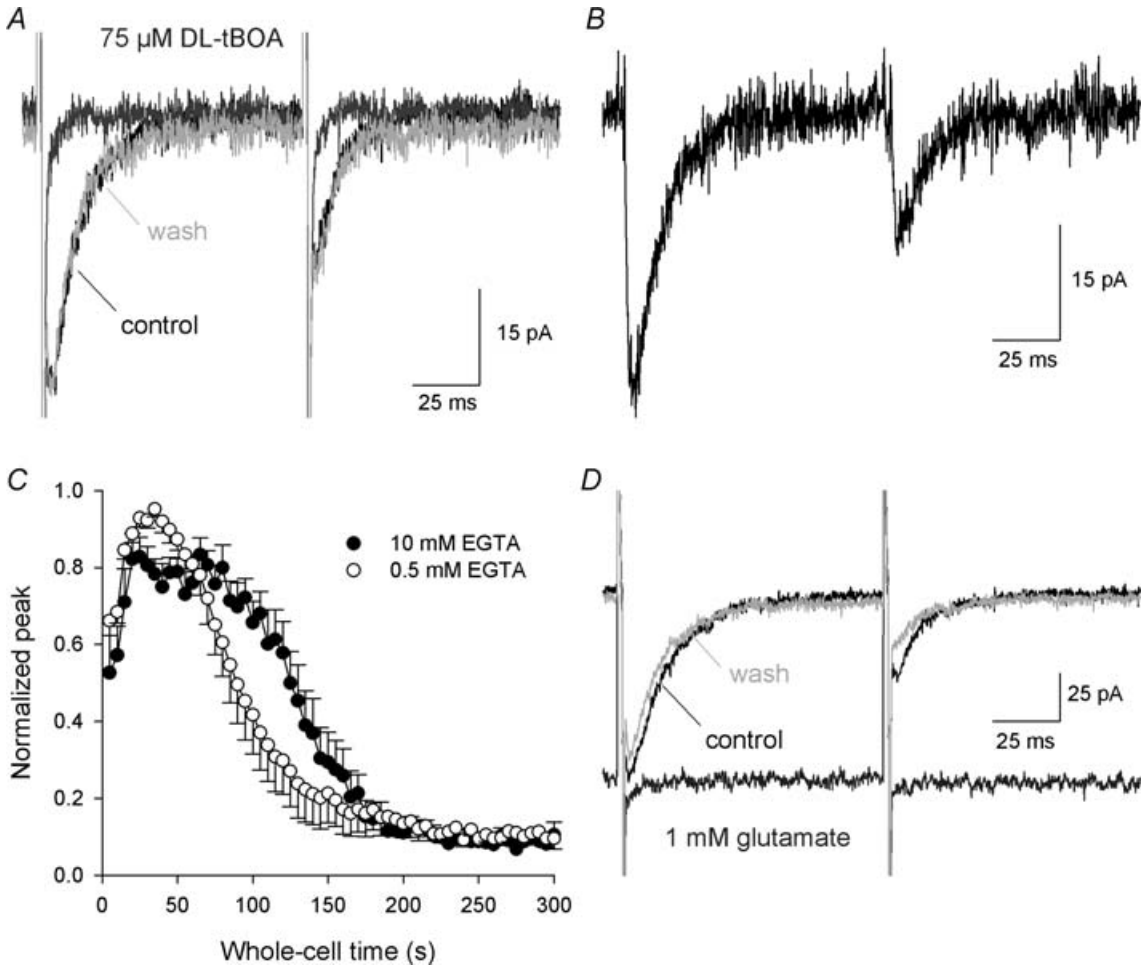

Figure 5. Characterization of the depolarization-evoked glutamate transporter current
A, paired (100 ms apart) 2 ms-depolarizations from -84 mV to -24 mV were given every 5 s. A 200 ms puff of 75 μm DL-tBOA applied in the vicinity of the axon terminals just before a paired depolarization blocked most of the transient current (dark grey trace). The transient current quickly recovered its initial amplitude (light grey trace). *B*, isolation of the DL-tBOA-sensitive transient current, by subtraction of the black and dark grey trace in *A*. *C*, peak amplitude of the depolarization-evoked currents as a function of the time after achieving the whole-cell configuration, normalized to the largest peak amplitude for the first depolarization, for either 10 mM ($n = 8$) or 0.5 mM intracellular EGTA ($n = 11$). The depolarization-evoked current was short-lived. It initially increased in the first 30 s, probably due to the change in internal Cl^- concentration. It started to decrease around 2 min in the whole-cell configuration and was undetectable after 4 min (*D*). The depolarization-evoked transient current can be saturated by application of glutamate (1 mM, 5 s puff, dark grey trace). The glutamate effect was washable (light grey trace). For clarity, cells used for *A*, *B* and *D* did not show GABA/glycinergic postsynaptic currents, but similar results were obtained from cells receiving synaptic inputs.

D-aspartate, confirming that they possessed functional glutamate transporters ($n = 3$, data not shown). These experiments confirmed that I_{trans} was dependent on Ca^{2+} influx through voltage-activated Ca^{2+} channels.

Comparison of the charge carried by I_{trans} and reciprocal inhibition

When the intracellular solution contained 10 mM EGTA, the observed IPSCs mostly corresponded to spontaneous rather than reciprocal inhibition synaptic events. The event frequency was not increased in the 100 ms following depolarization compared to baseline, and IPSCs could still be observed after the run-down of glutamate release (data not shown). The ratio of the current time integrals of I_{trans} and of the mean of the IPSCs was 2.1 ± 0.4 ($n = 10$ cells) for depolarizations evoking maximal I_{trans}. To increase the probability of monitoring reciprocal inhibition, we first decreased the EGTA concentration in the pipette to 0.5 mM. This induced an increase in the average I_{trans} first and second peak amplitudes from -69.7 ± 6.6 pA and -43.1 ± 3.9 pA with 10 mM EGTA to -100.6 ± 5.9 pA and -66.0 ± 5.2 pA with 0.5 mM EGTA. Consequently, the charge carried by I_{trans} increased from -531 ± 71 pA ms ($n = 10$) to -2074 ± 408 pA ms ($n = 6$), while the charge carried by a mean IPSC did not change (-317 ± 55 pA ms for 10 mM EGTA, -330 ± 108 pA ms for 0.5 mM EGTA). Lowering the EGTA in the pipette also had a tendency to accelerate the I_{trans} run-down (Fig. 5*C*), but not significantly ($P = 0.49$, repeated measurements ANOVA, $n = 9$ and 10 cells). Reciprocal inhibition was still not seen

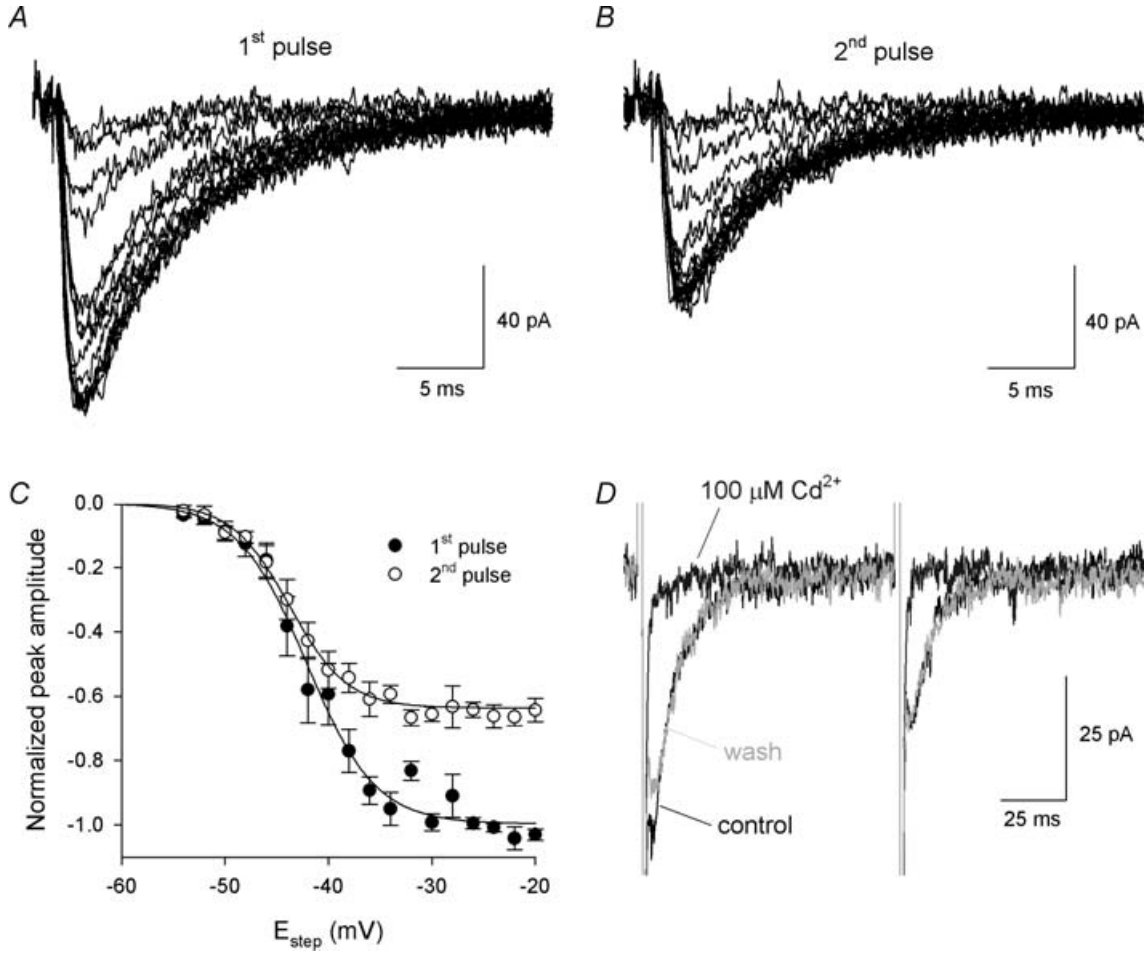

Figure 6. Voltage and Ca^{2+} current dependence of the depolarization-evoked currents
A and *B*, paired (100 ms apart) 2 ms depolarizations from −84 mV to a variable potential were given every second. The initial step voltage was −44 mV and was increased to −20 mV in 2 mV increments. The same protocol was applied in the absence then in the presence of 50 μM DL-tBOA (local puff starting 10 s before the 2nd protocol). The DL-tBOA-sensitive currents evoked by the first depolarization are shown in *A*, those by the paired depolarization in *B*. *C*, normalized peak amplitude as a function of the depolarization voltage ($n = 5$–7 depending on voltage). *D*, the depolarization-evoked transient current is blocked by a local application of 100 μM Cd^{2+} (dark grey trace). Puff duration was 15 s; the Cd^{2+} effect was washable (light grey trace).

following 2 ms depolarizations. Many studies in which reciprocal inhibition has been reported (Hartveit, 1999; Singer & Diamond, 2003; Vigh & von Gersdorff, 2005) used longer depolarizations and Cs^+/TEA rather than K^+-based internal solutions. We thus used a low EGTA (0.1 mM) Cs^+/TEA-based intracellular solution, including 5 mM glutamate, to try to slow down the run-down of I_{trans}. While 2 ms depolarization did evoke reciprocal inhibition in only 1 cell out of 14, longer depolarizations (12–52 ms in 10 ms steps) progressively evoked more reciprocal IPSCs as well as a longer slow phase (Fig. 7). IPSCs were blocked by a cocktail of 1 μM strychnine + 50 μM TPMPA + 100 μM bicuculline methiodide (Fig. 8*A* and *B*) allowing to isolate the noisy slow phase. On the other hand, puff application of 75 μM DL-tBOA inhibited the slow phase but not the IPSCs. For 50 ms depolarizations, the time integral of I_{trans} (slow phase) was 1.40 ± 0.15 time larger than the charge carried by reciprocal IPSCs (mean of the charge from 4 sweeps prior to inhibitory cocktail application) ($n = 4$ cells).

Discussion

EAAT5 localization in the mouse retina

In the mammalian retina, EAAT5 localization has been reported in the rat (Pow & Barnett, 2000; Pow *et al.* 2000), cat (Fyk-Kolodziej *et al.* 2004), rabbit and macaque retina (Pow *et al.* 2000). Rod photoreceptor terminals were labelled in all species, while expression in cone terminals was only confirmed in the cat retina, excluded in the macaque retina and remained uncertain in the rat and rabbit retina. RBC terminals as well as some cone bipolar cells were labelled in the adult rat retina (Pow & Barnett, 2000), while EAAT5 was not reported in rabbit, macaque and cat bipolar cells (Fyk-Kolodziej *et al.* 2004). In the cat retina, some amacrine and ganglion cells were labelled in addition to photoreceptors. We report here that in the mouse retina, EAAT5 is expressed in terminals of cone and rod photoreceptors. Cone pedicles were more strongly stained than rod spherules, a striking difference with the macaque retina. EAAT5 is also expressed in the axon and axon terminals of RBCs, most of the labelling in the INL and IPL colocalizing with the RBC-specific marker PKCα.

Glutamate transporters as postsynaptic receptors in the mammalian retina

Vertebrate photoreceptors continuously release glutamate in the dark and hyperpolarize in response to light, resulting in a decrease in glutamate release. This translates into the hyperpolarization of OFF bipolar cells via the closure of AMPA or kainate receptors (DeVries, 2000) and into the depolarization of ON bipolar cells via activation of mGluR6 metabotropic receptors (Slaughter & Miller, 1981; Nawy & Copenhagen, 1987). An additional glutamate-sensitive conductance has been reported on the dendrites of lower vertebrate ON bipolar cells (Saito *et al.* 1979; Kondo & Toyoda, 1980; Nawy & Copenhagen, 1987) and attributed to a glutamate transporter (Grant & Dowling, 1995, 1996; Wong *et al.* 2005). Previous studies of glutamate responses of mammalian bipolar cells did not report the existence of glutamate-dependent dendritic current besides the one controlled by mGluR6 (de la Villa *et al.* 1995; Euler *et al.* 1996). Hasegawa *et al.* (2006) recently reported that glutamate transporters did not contribute to the RBC response following rod depolarization. Thus the DL-tBOA-sensitive current of small amplitude that we observed following puff applications of glutamate on mouse RBC dendrites/soma most probably originates from non-synaptic EAAT5. It may rather arise from EAAT5 located on the RBC soma, as suggested by the immunolocalization data (Fig. 1 and Supplemental Fig. 1).

Glutamate transporters as presynaptic receptors in the mammalian retina

A presynaptic current with the characteristics of a transporter-associated current has been observed in lower vertebrate and mammalian photoreceptors (Sarantis *et al.* 1988; Tachibana & Kaneko, 1988; Picaud *et al.* 1995*b*; Hasegawa *et al.* 2006) and in goldfish bipolar cells (Palmer *et al.* 2003). Both EAAT2 and EAAT5 have been localized in photoreceptor terminals and in bipolar cells of the salamander (Eliasof *et al.* 1998), goldfish (Vandenbranden *et al.* 2000) and mammalian retina (Rauen *et al.* 1996; Pow & Barnett, 2000; Pow *et al.* 2000; Fyk-Kolodziej *et al.* 2004). However, EAAT2 has a small Cl^- conductance and is sensitive to dihydrokainate, while the currents reported here and from goldfish bipolar cell terminals were not (Palmer *et al.* 2003). Hence EAAT5, which is the glutamate transporter with the largest Cl^- conductance, is the most likely candidate to account for the currents reported in non-mammalian species and in the present study.

In mouse RBC, short depolarizations evoke a transient current that can be blocked either by the glutamate transporter inhibitor DL-tBOA (75 μM), or by the Ca^{2+} channel blocker Cd^{2+} (100 μM) or by removal of external Ca^{2+}. As expected from the release properties of bipolar cells from rats (Singer & Diamond, 2006) or lower vertebrates (von Gersdorff & Matthews, 1997; von Gersdorff *et al.* 1998; Palmer *et al.* 2003), a strong paired pulse depression was observed. The EAAT5 current may have been missed in previous studies for various reasons, the most obvious one being its fast rundown in whole-cell configuration. Classically, recordings in whole-cell mode are not performed right away after breaking into the cell, to allow enough time to achieve an equilibrium in the composition between the pipette medium and the intracellular compartment, and a proper compensation

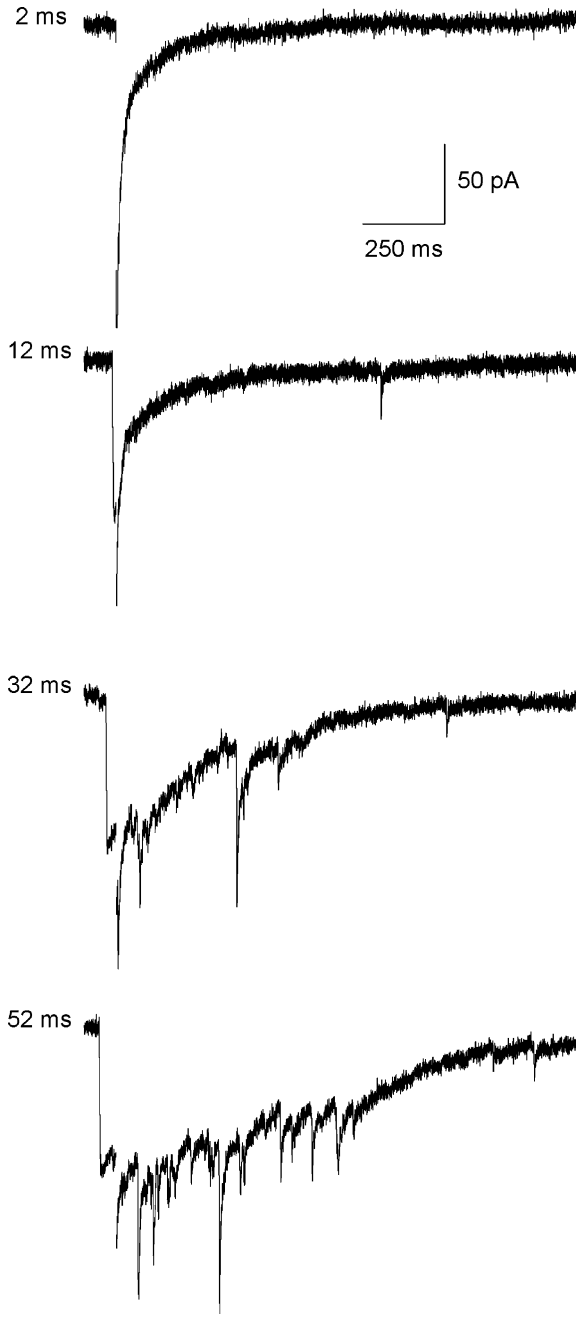

Figure 7. Reciprocal inhibition develops with depolarization duration
Representative traces of responses to depolarizations from −80 mV to −20 mV, obtained from the same RBC, with a low EGTA (0.1 mM) and Cs^+/TEA-based intracellular solution. The depolarization duration is indicated on the left of each trace. While only I_{trans} was observed for 2 ms depolarizations, the number of IPSCs increased with the depolarization duration.

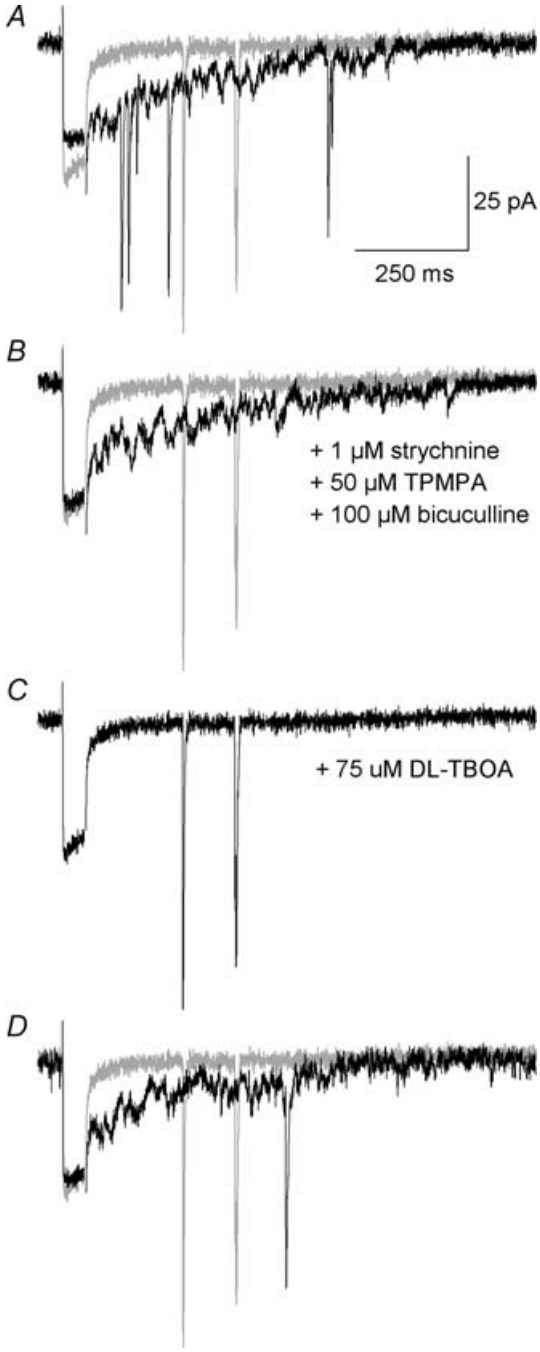

Figure 8. Pharmacology of the two components of inhibitory feedback
Following 50 ms depolarizations from −80 mV to −20 mV (repeated at 5 s intervals), a slow decaying current with superimposed IPSCs was observed upon repolarization in control conditions (*A* and *D*). IPSCs were blocked by a 10-s puff application of 1 μM strychnine + 50 μM TPMPA + 100 μM bicuculline methiodide (*B*) while the slow phase was inhibited by a 2 s puff application of 75 μM DL-tBOA (*C*). The 4 traces correspond to sweeps 2, 3, 5 and 8 of a recording from a RBC, with a low EGTA (0.1 mM) Cs^+/TEA-based intracellular solution. The sweep corresponding to blockade by DL-tBOA (*C*) was superimposed in grey on the other traces to facilitate a visual estimate of the charge carried by I_{trans} compared to the IPSCs.

for the membrane capacitance and access resistance. In addition, responses to glutamate were often envisaged from a dendritic point of view, glutamate being puffed in the vicinity of dendrites rather than on axon terminals. When considering feedback IPSCs in RBC terminals, this current if still present in the initial recordings could have been masked by long depolarizing pulses as in Hartveit (1999) and by K^+ channel tail current evoked by stronger depolarization when the repolarizing potential is far from E_K.

The depolarization-induced current was always smaller than the glutamate-evoked steady-state current, but still could be as large as 88% of its amplitude, indicating that most presynaptic transporters can be activated by the glutamate released following a single depolarization. This contrasts with what has been reported in the goldfish RBC, in which only 5% of the EAAT5-like glutamate transporters were activated by comparable depolarizations (Palmer *et al.* 2003).

It should be noted that in vertebrates, all reported transporters acting as presynaptic receptors were located at retinal glutamatergic ribbon synapses. Equivalent synapses exist in other sensory structures relying on graded potential neurons (e.g. auditory and vestibular hair cells) for which the localization of glutamate transporters has not been studied as thoroughly as in the retina. A fast and graded feedback directly linked to the transmitter release as the one offered by EAAT5 may be a common feature to these synapses, which have a higher rate of vesicular release than conventional synapses.

Role(s) of presynaptic EAAT5 in RBC

In mouse RBC axon terminals, E_{Cl} is close to -60 mV (Varela *et al.* 2005). Thus, EAAT5 will physiologically act as an inhibitory presynaptic receptor, opposing the terminal depolarization and providing a faster feedback than the one mediated by reciprocal synapses with amacrine cells. In conditions in which reciprocal inhibition could be monitored, the slower time course of the EAAT5 current makes it a larger charge carrier than inhibitory GABA and glycinergic inputs to the RBC terminals. It should be noted that, in those conditions, the glutamate release and clearance may have been affected. First, the Ca^{2+}-buffer used was weaker than the endogenous buffer, considered to be equivalent to 0.4 mM BAPTA or 2 mM EGTA (Burrone *et al.* 2002). Second, as K^+ was replaced by Cs^+ in the intracellular solution, the capacity of presynaptic EAAT5 to clear the glutamate from the synaptic cleft should be reduced as intracellular K^+ is required for proper glutamate transport. Both aspects should prolong I_{trans} and accentuate the amount of reciprocal inhibition received from amacrine cells, especially if EAAT5 is a key element in this clearance at RBC terminals, as recently reported for rod photoreceptors (Hasegawa *et al.* 2006). With K^+-based solutions and higher Ca^{2+} buffering capacities, especially for short depolarizations, the EAAT5 current should have an even more preponderant role in the feedback received by the RBC terminals.

Both GABA receptors and glutamate transporters can be modulated by PKC, which is highly expressed in RBCs (Greferath *et al.* 1990). While GABA receptors are down-regulated by PKC in rod bipolar cells (Feigenspan & Bormann, 1994; Gillette & Dacheux, 1996), PKC is expected to up-regulate glutamate transporters (Casado *et al.* 1993). Thus the exact balance between RBC auto-inhibition via EAAT5 and feedback from amacrine cells may vary depending on retinal activity.

The current-mediated action of EAAT5 can be strengthened by the fact that the charge carrier is Cl^-. Indeed, L-type Ca^{2+} channels in salamander rod photoreceptors can be modulated through a mechanism independent of G protein and phosphorylation (Kourennyi & Barnes, 2000), which may correspond to variations in the intracellular Cl^- concentration, a lower $[Cl^-]_i$ inhibiting Ca^{2+} entry (Thoreson & Stella, 2000; Thoreson *et al.* 2003). Following this line, Ca^{2+} channel inhibition by glutamate transporter activation reported in these cells can be explained through the EAAT5-mediated Cl^- efflux (Rabl *et al.* 2003). A similar mechanism can be considered in RBCs, which also express L-type Ca^{2+} channels on their axon terminals (de la Villa *et al.* 1998). The relative amplitude of I_{trans} compared to I_{Glu} suggests that the transporters are localized close to the release site, and thus close to the Ca^{2+} channels responsible for the Ca^{2+} entry controlling vesicular release. Thus, the impact of the Cl^- flux mediated by EAAT5 may be larger on Ca^{2+} channel activity than on the global Cl^- concentration in the terminal.

References

Arriza JL, Eliasof S, Kavanaugh MP & Amara SG (1997). Excitatory amino acid transporter 5, a retinal glutamate transporter coupled to a chloride conductance. *Proc Natl Acad Sci U S A* **94**, 4155–4160.

Auger C & Attwell D (2000). Fast removal of synaptic glutamate by postsynaptic transporters. *Neuron* **28**, 547–558.

Bagley EE, Gerke MB, Vaughan CW, Hack SP & Christie MJ (2005). GABA transporter currents activated by protein kinase A excite midbrain neurons during opioid withdrawal. *Neuron* **45**, 433–445.

Berntson A, Taylor WR & Morgans CW (2003). Molecular identity, synaptic localization, and physiology of calcium channels in retinal bipolar cells. *J Neurosci Res* **71**, 146–151.

Burrone J, Neves G, Gomis A, Cooke A & Lagnado L (2002). Endogenous calcium buffers regulate fast exocytosis in the synaptic terminal of retinal bipolar cells. *Neuron* **33**, 101–112.

Casado M, Bendahan A, Zafra F, Danbolt NC, Aragón C, Giménez C & Kanner BI (1993). Phosphorylation and modulation of brain glutamate transporters by protein kinase C. *J Biol Chem* **268**, 27313–27317.

de la Villa P, Kurahashi T & Kaneko A (1995). L-Glutamate-induced responses and cGMP-activated channels in three subtypes of retinal bipolar cells dissociated from the cat. *J Neurosci* **15**, 3571–3582.

de la Villa P, Vaquero CF & Kaneko A (1998). Two types of calcium currents of the mouse bipolar cells recorded in the retinal slice preparation. *Eur J Neurosci* **10**, 317–323.

Dehnes Y, Chaudhry FA, Ullensvang K, Lehre KP, Storm-Mathisen J & Danbolt NC (1998). The glutamate transporter EAAT4 in rat cerebellar Purkinje cells: a glutamate-gated chloride channel concentrated near the synapse in parts of the dendritic membrane facing astroglia. *J Neurosci* **18**, 3606–3619.

DeVries SH (2000). Bipolar cells use kainate and AMPA receptors to filter visual information into separate channels. *Neuron* **28**, 847–856.

Dudel J & Schramm M (2003). A receptor for presynaptic glutamatergic autoinhibition is a glutamate transporter. *Eur J Neurosci* **18**, 902–910.

Eliasof S, Arriza JL, Leighton BH, Kavanaugh MP & Amara SG (1998). Excitatory amino acid transporters of the salamander retina: identification, localization, and function. *J Neurosci* **18**, 698–712.

Eliasof S & Werblin F (1993). Characterization of the glutamate transporter in retinal cones of the tiger salamander. *J Neurosci* **13**, 402–411.

Euler T, Schneider H & Wässle H (1996). Glutamate responses of bipolar cells in a slice preparation of the rat retina. *J Neurosci* **16**, 2934–2944.

Fairman WA, Vandenberg RJ, Arriza JL, Kavanaugh MP & Amara SG (1995). An excitatory amino-acid transporter with properties of a ligand-gated chloride channel. *Nature* **375**, 599–603.

Feigenspan A & Bormann J (1994). Modulation of $GABA_C$ receptors in rat retinal bipolar cells by protein kinase C. *J Physiol* **481**, 325–330.

Fyk-Kolodziej B, Qin P, Dzhagaryan A & Pourcho RG (2004). Differential cellular and subcellular distribution of glutamate transporters in the cat retina. *Vis Neurosci* **21**, 551–565.

Ghosh KK, Bujan S, Haverkamp S, Feigenspan A & Wassle H (2004). Types of bipolar cells in the mouse retina. *J Comp Neurol* **469**, 70–82.

Gillette MA & Dacheux RF (1996). Protein kinase modulation of $GABA_A$ currents in rabbit retinal rod bipolar cells. *J Neurophysiol* **76**, 3070–3086.

Grant GB & Dowling JE (1995). A glutamate-activated chloride current in cone-driven ON bipolar cells of the white perch retina. *J Neurosci* **15**, 3852–3862.

Grant GB & Dowling JE (1996). On bipolar cell responses in the teleost retina are generated by two distinct mechanisms. *J Neurophysiol* **76**, 3842–3849.

Grant GB & Werblin FS (1996). A glutamate-elicited chloride current with transporter-like properties in rod photoreceptors of the tiger salamander. *Vis Neurosci* **13**, 135–144.

Greferath U, Grunert U & Wässle H (1990). Rod bipolar cells in the mammalian retina show protein kinase C-like immunoreactivity. *J Comp Neurol* **301**, 433–442.

Hartveit E (1999). Reciprocal synaptic interactions between rod bipolar cells and amacrine cells in the rat retina. *J Neurophysiol* **81**, 2923–2936.

Hasegawa J, Obara T, Tanaka K & Tachibana M (2006). High-density presynaptic transporters are required for glutamate removal from the first visual synapse. *Neuron* **50**, 63–74.

Kondo H & Toyoda JI (1980). Dual effect of glutamate and aspartate on the on-center bipolar cell in the carp retina. *Brain Res* **199**, 240–243.

Kourennyi DE & Barnes S (2000). Depolarization-induced calcium channel facilitation in rod photoreceptors is independent of G proteins and phosphorylation. *J Neurophysiol* **84**, 133–138.

Nawy S & Copenhagen DR (1987). Multiple classes of glutamate receptor on depolarizing bipolar cells in retina. *Nature* **325**, 56–58.

Otis TS, Kavanaugh MP & Jahr CE (1997). Postsynaptic glutamate transport at the climbing fiber-Purkinje cell synapse. *Science* **277**, 1515–1518.

Palmer MJ, Taschenberger H, Hull C, Tremere L & Von Gersdorff H (2003). Synaptic activation of presynaptic glutamate transporter currents in nerve terminals. *J Neurosci* **23**, 4831–4841.

Picaud SA, Larsson HP, Grant GB, Lecar H & Werblin FS (1995*b*). Glutamate-gated chloride channel with glutamate-transporter-like properties in cone photoreceptors of the tiger salamander. *J Neurophysiol* **74**, 1760–1771.

Picaud S, Larsson HP, Wellis DP, Lecar H & Werblin F (1995*a*). Cone photoreceptors respond to their own glutamate release in the tiger salamander. *Proc Natl Acad Sci U S A* **92**, 9417–9421.

Pow DV & Barnett NL (2000). Developmental expression of excitatory amino acid transporter 5: a photoreceptor and bipolar cell glutamate transporter in rat retina. *Neurosci Lett* **280**, 21–24.

Pow DV, Barnett NL & Penfold P (2000). Are neuronal transporters relevant in retinal glutamate homeostasis? *Neurochem Int* **37**, 191–198.

Rabl K, Bryson EJ & Thoreson WB (2003). Activation of glutamate transporters in rods inhibits presynaptic calcium currents. *Vis Neurosci* **20**, 557–566.

Rauen T, Rothstein JD & Wässle H (1996). Differential expression of three glutamate transporter subtypes in the rat retina. *Cell Tissue Res* **286**, 325–336.

Saito T, Kondo H & Toyoda JI (1979). Ionic mechanisms of two types of on-center bipolar cells in the carp retina. I. The responses to central illumination. *J General Physiol* **73**, 73–90.

Sarantis M, Everett K & Attwell D (1988). A presynaptic action of glutamate at the cone output synapse. *Nature* **332**, 451–453.

Singer JH & Diamond JS (2003). Sustained Ca^{2+} entry elicits transient postsynaptic currents at a retinal ribbon synapse. *J Neurosci* **23**, 10923–10933.

Singer JH & Diamond JS (2006). Vesicle depletion and synaptic depression at a mammalian ribbon synapse. *J Neurophysiol* **95**, 3191–3198.

Slaughter MM & Miller RF (1981). 2-Amino-4-phosphonobutyric acid: a new pharmacological tool for retina research. *Science* **211**, 182–185.

Sonders MS & Amara SG (1996). Channels in transporters. *Curr Opin Neurobiol* **6**, 294–302.

Tachibana M & Kaneko A (1988). L-Glutamate-induced depolarization in solitary photoreceptors: a process that may contribute to the interaction between photoreceptors in situ. *Proc Natl Acad Sci U S A* **85**, 5315–5319.

Thoreson WB, Bryson EJ & Rabl K (2003). Reciprocal interactions between calcium and chloride in rod photoreceptors. *J Neurophysiol* **90**, 1747–1753.

Thoreson WB & Stella SL (2000). Anion modulation of calcium current voltage dependence and amplitude in salamander rods. *Biochim Biophys Acta* **1464**, 142–150.

Vandenbranden CA, Yazulla S, Studholme KM, Kamphuis W & Kamermans M (2000). Immunocytochemical localization of the glutamate transporter GLT-1 in goldfish (*Carassius auratus*) retina. *J Comp Neurol* **423**, 440–451.

Varela C, Blanco R & De la Villa P (2005). Depolarizing effect of GABA in rod bipolar cells of the mouse retina. *Vision Res* **45**, 2659–2667.

Vigh J & Von Gersdorff H (2005). Prolonged reciprocal signaling via NMDA and GABA receptors at a retinal ribbon synapse. *J Neurosci* **25**, 11412–11423.

von Gersdorff H & Matthews G (1997). Depletion and replenishment of vesicle pools at a ribbon-type synaptic terminal. *J Neurosci* **17**, 1919–1927.

von Gersdorff H, Sakaba T, Berglund K & Tachibana M (1998). Submillisecond kinetics of glutamate release from a sensory synapse. *Neuron* **21**, 1177–1188.

Wong KY, Cohen ED & Dowling JE (2005). Retinal bipolar cell input mechanisms in giant danio. II. Patch-clamp analysis of on bipolar cells. *J Neurophysiol* **93**, 94–107.

Acknowledgments

This work was supported by Human Frontier grant RGY0004-2003 to M.J.R., an Association Française contre les Myopathies fellowship to E.W., INSERM and CNRS. We thank Prof. Pierre Chambon for hosting M.J.R. and E.W. at the Mouse Clinical Institute (Illkirch, France) and Dr. Stéphane Supplisson and Carolina Varela for valuable comments on the manuscript.

Supplemental material

The online version of this paper can be accessed at:
DOI: 10.1113/jphysiol.2006.118828
http://jp.physoc.org/cgi/content/full/jphysiol.2006.118828/DC1
and contains supplemental material consisting of three figures.

Supplemental Figure 1. EAAT5 is expressed in rod bipolar cells

Supplemental Figure 2: Pharmacology of the glutamate-induced current

Supplemental Figure 3: Glutamate evokes a current on both the dendrites/soma and axon terminals of rod bipolar cells

This material can also be found as part of the full-text HTML version available from http://www.blackwell-synergy.com